AZD9291, an irreversible EGFR TKI, overcomes T790M-mediated resistance to EGFR inhibitors in lung cancer

Darren A. E. Cross[1], **Susan E. Ashton**[1], **Serban Ghiorghiu**[1], **Cath Eberlein**[1], **Caroline A. Nebhan**[3], **Paula J. Spitzler**[3], **Jonathon P. Orme**[2], **M. Raymond V. Finlay**[1], **Richard A. Ward**[1], **Martine J. Mellor**[1], **Gareth Hughes**[1], **Amar Rahi**[1], **Vivien N. Jacobs**[1], **Monica Red Brewer**[3], **Eiki Ichihara**[3], **Jing Sun**[3], **Hailing Jin**[3], **Peter Ballard**[1], **Katherine Al-Kadhimi**[1], **Rachel Rowlinson**[1], **Teresa Klinowska**[1], **Graham H. P. Richmond**[1], **Mireille Cantarini**[1], **Dong-Wan Kim**[4], **Malcolm R. Ranson**[5], and **William Pao**[3]

[1]AstraZeneca Oncology Innovative Medicines, Alderley Park, Macclesfield Cheshire, SK10 4TG, United Kingdom

[2]Discovery Sciences, Mereside, Alderley Park, Macclesfield Cheshire, SK10 4TG, United Kingdom

[3]Department of Medicine and Vanderbilt-Ingram Cancer Center, Vanderbilt University, Nashville, TN 37232 USA

[4]Seoul National University Hospital, Seoul, Republic of Korea

[5]University of Manchester, Christie Hospital, Manchester, M20 4BX, United Kingdom

Abstract

First generation EGF receptor tyrosine kinase inhibitors (EGFR TKIs) provide significant clinical benefit in patients with advanced EGFR mutant (EGFRm+) non-small cell lung cancer (NSCLC). Patients ultimately develop disease progression, often driven by acquisition of a second T790M EGFR TKI resistance mutation. AZD9291 is a novel oral, potent and selective third generation irreversible inhibitor of both EGFRm+ sensitizing and T790M resistance mutants that spares wild-type EGFR. This monoanilino-pyrimidine compound is structurally distinct from other third generation EGFR TKIs and offers a pharmacologically differentiated profile from earlier

generation EGFR TKIs. Pre-clinically, the drug potently inhibits signaling pathways and cellular growth in both EGFRm+ and EGFRm+/T790M mutant cell lines *in vitro*, with lower activity against wild-type EGFR lines, translating into profound and sustained tumor regression in EGFR mutant tumor xenograft and transgenic models. The treatment of two patients with advanced EGFRm T790M+ NSCLC is described as proof of principle.

Introduction

Gefitinib (1) and erlotinib (2) are reversible small molecule ATP analogues originally designed to inhibit the tyrosine kinase (TK) activity of wild-type epidermal growth factor receptor (EGFR). During their clinical development, these first-generation TK inhibitors (TKIs) were serendipitously found to be most effective in advanced non-small cell lung cancer (NSCLC) patients whose tumors harbor recurrent somatic activating mutations occurring in the exons encoding the kinase domain of EGFR, i.e. small multi-nucleotide in-frame deletions in exon 19 (ex19del) and a point mutation in exon 21 leading to substitution of leucine for arginine at position 858 (L858R) (3-5). Tumors with these activating mutations (EGFRm+) account for approximately 10-15% and 40% of NSCLC in Western and Asian populations respectively (6). Unfortunately, whilst patients with EGFRm+ tumors typically show good initial responses to first generation TKIs, most patients who respond to therapy ultimately develop disease progression after about 9-14 months of treatment (7-11). Furthermore, these first generation TKIs are associated with side effects that include skin rash and diarrhea that are due to the inhibition of wild-type EGFR in skin and gastrointestinal organs (12).

Preclinical modeling and analysis of tumor tissue obtained from patients after the development of disease progression has led to the identification of a number of mechanisms that mediate EGFR TKI resistance. Such genetic and other signaling aberrations that drive resistance mechanisms include HER2 amplification (13), MET amplification (14, 15), PIK3CA mutation (16), BRAF mutation (17), NF1 loss (18) and potentially FGFR signaling (19). In addition, resistant tumors have also been reported to show histologic changes such as small cell lung cancer (SCLC) transformation or epithelial mesenchymal transition (EMT) (16). However, it is now well established that acquisition of a second mutation in EGFR, resulting in substitution of threonine at the "gatekeeper" amino acid 790 to methionine (T790M) is the most common resistance mechanism and is detected in tumor cells from more than 50% of patients after disease progression (20, 21). The T790M mutation is believed to render the receptor refractory to inhibition by these reversible EGFR TKIs through exerting effects on both steric hindrance (22) and increased ATP affinity (23).

Current targeted therapeutic strategies for patients with acquired resistance are limited. Second-generation irreversible EGFR TKIs such as afatinib (24) and dacomitinib (25) are effective in untreated EGFR mutant lung cancer (26, 27). However, as monotherapy, they

have failed to overcome T790M-mediated resistance in patients (28, 29), because concentrations at which these irreversible TKIs overcome T790M activity pre-clinically are not achievable in humans due to dose-limiting toxicity related to non-selective inhibition of wild-type EGFR (30). Furthermore, these inhibitors can drive resistance through acquisition of T790M *in vitro* (31) and in patients (32), providing supportive evidence that they have low potency against T790M. One regimen that showed potential activity is afatinib plus the anti-EGFR antibody, cetuximab, which induced a 32% unconfirmed response rate in a phase IB trial for patients with EGFRm+ lung cancer and acquired resistance to erlotinib (33). However, this combination has substantial skin toxicity with 18% of patients reporting CTCAE grade 3 or higher rash (33).

Therefore, there remains a significant unmet need for an EGFR TKI agent that can more effectively target T790M tumors while sparing the activity of wild-type EGFR. This has led to the development of "third generation" EGFR TKIs that are designed to target T790M and EGFR TKI-sensitizing mutations more selectively than wild-type EGFR. WZ4002 was the first such agent to be published (34), although it has not progressed to clinical trials. A second agent closely related to the WZ4002 series, CO-1686, has been recently reported (35), and is currently in early Phase II clinical trials. HM61713 is another "third generation" agent that is currently in early Phase I trials.

Here, we describe identification, characterization, and early clinical development of AZD9291, a novel, irreversible, EGFR TKI with selectivity against mutant versus wild-type forms of EGFR. AZD9291 is a mono-anilino-pyrimidine compound that is structurally and pharmacologically distinct from all other TKIs including CO-1686 and WZ4002.

Results

AZD9291 is a mutant-selective, irreversible inhibitor of EGFR kinase activity

AstraZeneca developed a novel series of irreversible, small-molecule inhibitors to target the sensitizing and T790M resistant mutant forms of the EGFR tyrosine kinase with selectivity over the wild-type form of the receptor. These compounds bind to the EGFR kinase irreversibly by targeting the cysteine-797 residue in the ATP binding site via covalent bond formation (36), as depicted in the modeling structure for AZD9291 **(Fig. 1A)**. Further work on this chemotype allowed additional structure activity relationships (SAR) to be discerned that enabled target potency to be increased without driving increased lipophilicity, thus maintaining favorable drug-like properties. Continued medicinal chemistry efforts achieved further improvements including increased kinase selectivity, ultimately arriving at the mono-anilino-pyrimidine AZD9291 **(Fig. 1B)**. Mass spectrometry of chymotrypsin digests confirmed that AZD9291 can covalently modify recombinant EGFR (L858R/T790M) at the target cysteine 797 amino acid **(Supplementary Fig. S1 A&B)**.

AZD9291 has a distinct chemical structure from the other third-generation TKIs, WZ4002 (34) and CO-1686 (35). Whilst the former two compounds share a number of common structural features (e.g. positioning of the electrophilic functionality that undergoes reaction with a conserved cysteine residue present in EGFR (Cys 797), heteroatom-linked pyrimidine 4-substituents, and presence of a pyrimidine 5-substituent), AZD9291 is architecturally

unique. Amongst other differences, the electrophilic functionality resides on the pyrimidine C-2 substituent ring, the pyrimidine 4-substituent is C-linked and heterocyclic, and the pyrimidine 5-position is devoid of substitution.

In EGFR recombinant enzyme assays (Millipore), AZD9291 showed an apparent IC_{50} of 12 nM against L858R and 1 nM against L858R/T790M; these are called apparent since the amount of active enzyme changes over time and thus IC_{50} is time-dependent for irreversible agents. The drug exhibited nearly 200 times greater potency against L858R/T790M than wild-type EGFR **(Supplementary Table S1A)**, consistent with the design goal of a mutant EGFR selective agent in comparison to early generation TKIs. Subsequent murine *in vivo* studies revealed that AZD9291 was metabolized to produce at least two circulating metabolite species, AZ5104 and AZ7550. In biochemical assays, AZ7550 had a comparable potency and selectivity profile to the parent **(Supplementary Table S1A)**. In contrast, although AZ5104 exhibited the same overall profile, it was more potent against mutant and wild-type EGFR forms, thus demonstrating a smaller selectivity margin compared to parent **(Supplementary Table S1A)**.

To explore a broader kinome selectivity profile, we tested AZD9291 and metabolites at 1 μM across approximately 280 other kinases available on a commercial biochemical kinome panel (Millipore). AZD9291 showed minimal off-target kinase activity, with only a limited number of additional kinases showing greater than 60% inhibition at 1 μM and moderate IC_{50} potencies such as ErbB2/4, ACK1, ALK, BLK, BRK, MLK1 and MNK2 **(Supplementary Table S1B)**. The active metabolites displayed a similar secondary target profile as parent **(Supplementary Table S1B)**. Given that AZD9291 makes a covalent bond with Cys797 in EGFR as described, we were specifically interested to explore potency in other kinases that have a cysteine residue in the analogous kinase domain position. Of the nine other kinases present within the human kinome with the analogous Cys797 to EGFR, AZD9291 showed significant activity only in a biochemical assay against ErbB2, ErbB4 and BLK **(Supplementary Table S1B)**, supporting the overall high degree of selectivity that AZD9291 confers.

Like the T790M double-mutant EGFR receptor, the insulin-like growth factor receptor (IGF-1R) and insulin receptor (IR) also have a methionine gatekeeper in their kinase domains. We considered it important to develop selectivity against these kinases to minimize potential dose limiting toxicities related to hyperglycaemia. Using a commercially available cellular IGF-1R phosphorylation assay as a surrogate, AZD9291 and the metabolite AZ5104 did not exhibit significant activity towards this receptor family **(Supplementary Table S1C)**. Moreover, a single oral dose of 200 mg/kg of AZD9291 in rats did not cause a significant change in blood glucose or insulin levels over a 24 hour period, consistent with lack of IGF-1R activity (data not shown).

Finally, we evaluated cellular potency against HER2 (ErbB2), using three different cellular approaches: surrogate kinase assays involving expression of wild-type HER2 in HEK293 cells **(Supplementary Fig. S2A)**, PC-9 cells (ex19del) engineered to overexpress HER2 **(Supplementary Fig. S2B**; (13) and biochemical reconstitution studies in HEK293 cells involving intracellular domain constructs encoding L858R/T790M, wild-type EGFR, or

wild-type HER2 (**Supplementary Fig. S2C**; (37). Consistently, treatment of cells with AZD9291 inhibited phosphorylation of HER2 at moderate potency levels. However, consistent with its greater wild-type EGFR potency, the AZ5104 metabolite showed more potency than AZD9291 against phospho-HER2 (**Supplementary Fig. S2A-C**).

AZD9291 potently and selectively targets mutant EGFR cell lines *in vitro*

We compared AZD9291 with other early generation EGFR TKIs in EGFR phosphorylation and cell death (Sytox) assays using a number of tumor cell lines harboring either wild-type or different forms of mutant EGFR. Compared with other EGFR inhibitors of both first (gefitinib and erlotinib) and second generation (afatinib and dacomitinib), AZD9291 demonstrated a unique third generation TKI profile. AZD9291 showed similar potency to early generation TKIs in inhibiting EGFR phosphorylation in EGFR cells harboring sensitising EGFR mutants including PC-9 (ex19del), H3255 (L858R) and H1650 (ex19del) **(Fig. 2A),** with mean IC_{50} values ranging from 13 to 54 nM for AZD9291. AZD9291 also potently inhibited phosphorylation of EGFR in T790M mutant cell lines (H1975 (L858R/T790M), PC-9VanR (ex19del/T790M) **(Fig. 2A)**, with mean IC_{50} potency less than 15 nM. First generation reversible TKIs were ineffective at inhibiting phosphorylation of T790M EGFR **(Fig. 2A)**. The second generation irreversible TKIs, afatinib and dacomitinib, showed activity against T790M EGFR *in vitro*, although this activity is may not be achievable at exposures that can be reached in the clinic. AZD9291 was less potent at inhibiting phosphorylation of EGFR in wild-type cell lines (A431, LOVO, NCI-H2073), with mean IC_{50} range of 480 to 1865 nM **(Fig. 2A)**. This is in clear contrast to the early generation TKIs which all potently inhibited EGFR phosphorylation in wild-type lines with similar potency to sensitizing-mutant EGFR **(Fig. 2A)**. Similar results were found when phosphorylation of EGFR and downstream signaling was determined by immunoblot analysis of lysates from PC-9, H1975, LOVO, H1650 and H3255 lines **(Fig. 2B)**. Consistently, results showed that AZD9291 more potently inhibited phospho-EGFR and downstream signaling substrates (pAKT, pERK) in cells with mutant EGFR compared with wild-type **(Fig. 2B),** although H1650 cells retained higher phospho-AKT levels due to loss of PTEN (38).

As previously described, AZD9291 has active circulating metabolites, so we also profiled their activity against EGFR. Consistent with presented biochemical data, AZ7550 exhibited very similar potency and profile to AZD9291 against mutant and wild-type cell lines tested **(Supplementary Table S1D)**, whilst AZ5104 harbored somewhat greater potency against ex19del (2 nM in PC-9), T790M (2 nM in H1975) and wild-type EGFR (33 nM in LOVO) cell lines. Therefore, AZ5104 exhibited a reduced selectivity margin against wild-type EGFR when compared to AZD9291. However, taken together, this mechanistic data confirmed the third generation TKI properties of AZD9291 compared to earlier generation agents: equivalent activity against sensitizing mutant EGFR, superior activity towards T790M and increased selectivity margin against wild-type EGFR.

We then explored how the pharmacological activity against mutant and wild-type EGFR signaling translated into cell proliferation effects using a Sytox live/dead cell phenotype endpoint. In line with the phosphorylation data, AZD9291 showed high levels of phenotype

potency in both sensitizing-mutant (mean IC_{50} of 8 nM in PC-9) and T790M (mean IC_{50} of 11 and 40 nM in H1975 and PC-9VanR respectively) EGFR cell lines, whilst having much less activity towards wild-type EGFR (mean IC_{50} of 650 and 461 nM in Calu3 and H2073 respectively) **(Fig. 3A)**. Again, this contrasted to second generation TKIs, afatinib and dacomitinib, which showed much less activity against T790M lines and were associated with much greater potency towards wild-type EGFR **(Fig. 3A).** To confirm these results, we determined the efficacy of AZD9291 in an independent laboratory against a panel of isogenic pairs of drug-sensitive /resistant EGFR mutant lung cancer cell lines (31, 39). Parental EGFRm+ lines (PC-9, H3255, HCC827, HCC4006, 11-18) were sensitive to AZD9291 as well as erlotinib, afatinib, and AZD8931 (a reversible equipotent inhibitor of EGFR, HER2 and HER3 signalling (40)) **(Fig. 3B)**. However, only AZD9291 displayed low nanomolar activity against the lines harboring EGFR T790M (H1975, HCC827/ER1, PC-9/BRc1 and H3255/XLR) **(Fig. 3B)**. Interestingly, AZD9291 was not effective against lines harboring non-T790M resistance such as 11-18/ER (NRAS), HCC827/ER2 (MET amplification), and HCC4006/ER (EMT) (17) **Fig. 3B)**. In a separate large cell panel proliferation profiling study, AZD9291 was also poorly active *in vitro* (IC50 ~1 μM) against both NSCLC NCI-H820 and EBC-1 cell lines that harbor MET amplification and mutant EGFR (data not shown). Consistent with phospho-EGFR data, the metabolite AZ5104 again demonstrated much greater potency across cell lines in a phenotypic assay, whereas AZ7550 was broadly similar, with the same overall profile maintained **(Supplementary Table S1E)**.

Due to their low activity against T790M EGFR, it has been suggested that treatment with early generation TKIs can induce the growth selection of tumor cells harboring EGFRm+/T790M leading to TKI resistant populations both pre-clinically and clinically (31). We therefore hypothesized that such resistance would not occur upon treatment with AZD9291, given its superior potency against T790M. Indeed, whilst chronic treatment with gefitinib or afatinib commonly caused acquired resistance in PC-9 cells *in vitro* through gain of T790M, acquired resistance to AZD9291 through T790M was not observed **(Fig. 3C)**. Studies are ongoing to characterize the T790M independent mechanisms of acquired resistance to AZD9291 (Eberlein et al., manuscript in preparation).

Activity of AZD9291 against rare EGFR and HER2 mutants *in vitro*

In addition to activity against the common activating/sensitizing EGFR mutants, we assessed the potency of AZD9291 against other rarer EGFR mutants associated with sensitivity or resistance to first-generation EGFR TKIs **(Supplementary Fig. S3)**. 293 cells were transfected with cDNAs encoding EGFR G719S, L861Q, an exon 20 insertion (H773-V774HVdup), exon 19 insertion (I744-K745insKIPVAI) or an EGFR variant III (EGFRvIII; found in brain glioblastomas (41)), and treated with increasing concentrations of either erlotinib, afatinib, AZD9291, the metabolite AZ5104, or AZD8931 for 6 hours. Immunoblotting was performed on corresponding lysates using antibodies against phospho-EGFR (Y1173) and total EGFR. All EGFR TKIs were effective against EGFR L861Q (consistent with kinase profiling data **(Table 1)**), G719S, and the exon 19 insertion, although AZD9291 was somewhat less potent compared with the AZ5104 metabolite against these mutant EGFR forms **(Supplementary Figure S3A)**. None of the TKIs was effective against the exon 20 insertion mutation **(Supplementary Figure S3B)**. For the EGFRvIII mutant,

AZD9291 demonstrated lower potency compared to afatinib and AZD8931. AZ5104, however displayed a higher level of activity **(Supplementary Figure S3C)**. These data are consistent with the kinase activity of the vIII mutant being similar to that of their wild-type EGFR.

We similarly explored activity against HER2 mutations found in NSCLC. Compared to afatinib and AZ5104, AZD9291 exhibited moderate potency against H1781 cells, which harbor a VC insertion at G776 in exon 20 of *HER2* (42), with an IC50 of 80 nM **(Supplementary Fig. S4A)**. However, AZD9291 was more effective at inhibiting growth of these cells than erlotinib. The effect of various TKIs on HER2-associated signaling in H1781 cells was consistent with these results **(Supplementary Fig. S4B)**. Similar activity was observed in 293 cell transfectants harboring the most common HER2 mutant in NSCLC (exon20 YVMA 776-779ins) (43) **(Supplementary Fig. S4C)**. Thus, in patients, AZD9291 and its metabolite AZ5104, may also be able to target HER2 in tumors, depending on the clinical exposures that are achieved.

AZD9291 causes profound and sustained regression in mutant EGFR *in vivo* xenograft models

AZD9291 demonstrated good bioavailability, was widely distributed in tissues, and had moderate clearance resulting in a half-life of around 3 hours after oral dosing in the mouse **(Supplementary Fig. S5)**. The circulating active metabolites in plasma each had a similar half-life, and the total exposure levels (AUC) were approximately 68 and 33% compared to the parent compound for AZ7550 and AZ5104, respectively **(Supplementary Fig S5)**.

To explore *in vivo* activity of AZD9291, we administered the drug as monotherapy against various mutant EGFR xenografts representing clinical NSCLC settings. Once daily dosing of AZD9291 induced significant dose-dependent regression in both PC-9 (ex19del) and H1975 (L858R/T790M) tumor xenograft models, with tumor shrinkage observed at doses as low as 2.5mg/kg/day in both models after 14 days **(Fig. 4A, B)**. Similar tumor shrinkage was seen after administration of 5 mg/kg/day AZD9291 in H3255 (L858R) **(Supplementary Fig. S6A)** and PC-9VanR (ex19 del/ T790M) **(Supplementary Fig. S6B)** xenografts after 14 days. These studies showed that AZD9291 can induce profound shrinkage at low doses against both EGFR drug-sensitizing and T790M-resistant EGFR mutant disease models.

We next explored the durability of tumor shrinkage. Chronic long term daily oral dosing of AZD9291 resulted in complete and durable macroscopic responses of both PC-9 **(Fig. 4C)** and H1975 xenografts **(Fig. 4D)**. For PC-9 cells, no visible tumors were evident following 40 daily doses with 5 mg/kg of AZD9291 in 8 of 8 tumors, and this complete response was sustained out to 200 days when the study was terminated (data not shown). As a comparison, gefitinib at 6.25 mg/kg/day, a clinically representative dose, induced less tumor regression, and tumors began to re-grow after approximately 90 days. In H1975 xenografts, 5 mg/kg/day AZD9291 resulted in complete responses in 10 of 12 tumors. Re-growth was observed after approximately 50 days treatment with 1 mg/kg/day, but an increased dose of 25 mg/kg/day AZD9291 re-induced tumor regression possibly suggesting re-growth was still driven by T790M EGFR. No visible tumors were evident after 20 days dosing of 25

mg/kg/day AZD9291 in the H1975 xenograft model. Moreover, the complete responses were maintained for the duration of the study period with no evidence of tumor progression during 200 days of treatment. No growth was observed for an additional 30 days after treatment was stopped. AZD9291 daily dosing was well tolerated in the animals with minimal body weight loss, (less than 5% of starting body weight) even after dosing for 200 days **(Supplementary Fig. S6C (PC-9) and S6D (H1975))**. Similar long term dosing studies were performed in the H3255 model, with 5 mg/kg/day AZD9291 causing non-measurable tumors in all 8 dosed mice by day 53. By contrast, only one mouse treated with 6.25 mg/kg gefitinib achieved non-measurable tumor status **(Supplementary Fig. S6A)**.

To explore comparative efficacy against wild-type EGFR, AZD9291 was tested in A431 xenografts. These cells are used as a model for wild-type EGFR activity, but they are highly dependent on amplified wild-type EGFR and therefore are unlikely to reflect normal tissue EGFR pharmacology/physiology (44). AZD9291 did induce some moderate tumor growth inhibition at 5 mg/kg/day **(Supplementary Fig. S6E)**, suggesting AZD9291 or associated metabolites are not entirely inactive against wild-type EGFR in this model. By contrast, this same 5 mg/kg/day dose level was sufficient to induce profound and sustained tumor shrinkage in both H1975 and PC-9 mutant EGFR tumor xenograft models **(Figs. 4A-B)**, consistent with AZD9291 having a significant selectivity margin over wild-type EGFR.

AZD9291 causes profound and sustained regression in mutant EGFR *in vivo* transgenic tumor models

We further examined tumor responses in previously generated mouse tumor models that develop lung adenocarcinomas driven by $EGFR^{L858R}$ (45) or $EGFR^{L858R + T790M}$ (46). These models employ a tetracycline–inducible (tet-inducible) system, involving bitransgenic animals. One transgene carries a tet transactivator in lung epithelia (i.e., Clara cell secretory protein – reverse tetracycline transactivator [CCSP-rtTA], herein referred to as "C" mice). The 2 relevant strains are referred to as C/L858R and C/L+T, respectively. As expected, tumors harboring $EGFR^{L858R}$ were sensitive to erlotinib, while tumors expressing $EGFR^{L858R + T790M}$ were resistant (46). Here, we treated tumor-bearing mice with AZD9291 (5 mg/kg/day), afatinib (7.5 mg/kg/day), or vehicle control for one to two weeks. Within days of treatment, 5 of 5 C/L858R mice displayed nearly 80% reduction in tumor volume by magnetic resonance imaging MRI (see Methods and (47)) after therapy with both afatinib or AZD9291, while 5 of 5 mice treated with vehicle showed tumor growth **(Figs. 5A (top) and 5B)**. Upon histological examination, only vehicle-treated mice showed viable tumor **(Fig. 5B)**. By contrast, in C/L+T animals, only AZD9291 treatment induced significant tumor shrinkage **(Figs. 5A (middle&bottom) and 5C)**, while both vehicle- and afatinib-treated mice showed viable tumor **(Fig. 5C)**. The difference in tumor responses was more pronounced after 2 weeks of treatment **(Fig. 5A (bottom))**. Furthermore, preliminary data in a single mouse with tumor driven by an ex19del mutant alone (45) also responded rapidly to AZD9291 **(Supplementary Fig. S7A)**. The metabolite, AZ5104 (5 mg/kg/day), was also effective in shrinking tumors in both C/L858R **(Supplementary Fig. S7B, C)** and C/L+T mice **(Supplementary Fig. S7B, D)**.

Pharmacodynamic confirmation of target inhibition by AZD9291

To confirm on-target and pathway activity of AZD9291, we examined tumor tissues from the H1975 xenograft and L858R/T790M transgenic model after drug treatment. Mice bearing H1975 xenografts were given a single dose of AZD9291 (5 mg/kg) and tumors were harvested 1, 6, 16, 24, and 30 hours later. Sections from formalin-fixed paraffin-embedded tumors were then stained for the phosphorylated forms of-EGFR (Tyr1173), ERK (Thr202/Tyr204), S6 (Ser235/236), and PRAS40 (Thr246). In the H1975 model, AZD9291 treatment strongly inhibited both phospho-EGFR and downstream signalling pathways after 6 hours **(Fig. 6A)**. Although in mice, the pharmacokinetic half-life of AZD9291 is only ~3 hours, phospho-EGFR staining remained significantly diminished even after the 30 hour time point, consistent with its expected irreversible mode of action. Interestingly, although downstream signaling molecules similarly showed maximal inhibition after 6 hours, in contrast to phospho-EGFR, they displayed more transient inhibition **(Fig. 6A)**.

In the transgenic model, we similarly observed target inhibition after 5mg/kg dosing of AZD9291 via immunohistochemical staining of sections for phospho-EGFR and downstream markers **(Fig. 6B)** or immunoblotting of lysates **(Fig. 6C)** from treated tumors.

Proof of principle clinical activity of AZD9291 in patients with acquired resistance to EGFR TKIs

The mesylate salt of AZD9291 is currently in a first-in-human phase I dose escalation clinical trial (AURA; NCT01802632; AstraZeneca) in patients with advanced EGFRm+ NSCLC who had disease progression following treatment with any EGFR TKI (including gefitinib or erlotinib). As proof-of-principle, here we present preliminary results of the first two patients in the study with confirmed radiographic responses (as per RECIST 1.1 (48) treated at the lowest dose cohort (20 mg once daily) **(Fig. 7)** (49). Both patients' tumors harbored drug sensitive EGFR mutations in addition to documented T790M mutations (according to local testing results). Consistent with AZD9291 being less active against wild-type EGFR, in these two cases there were no rash events and only one reported CTCAE Grade 1 diarrhea. Preliminary clinical pharmacokinetic analysis indicates that AZD9291, AZ5104 and AZ7550 have a half-life of at least 50 hours, longer than would be predicted from the preclinical data, which results in a desirable flat PK profile after multiple once daily dosing **(Fig 7A)**. Further Phase 1 clinical data for this study will be submitted for publication at a later date.

The first patient was a 57-year old East Asian female patient from South Korea diagnosed with Stage IV EGFR mutant (ex 19 del) NSCLC in May 2011. The patient had disease progression following 2 cycles of gemcitabine plus carboplatin combination chemotherapy. The patient next had a partial response on gefitinib before developing disease progression after 10 months. She then had stable disease with 4 cycles of pemetrexed followed by 4 cycles of paclitaxel plus carboplatin with a best response of partial response before progressing immediately before study. Analysis of tumor tissue, from a biopsy taken immediately before AZD9291 study entry, using direct dideoxynucleotide-based sequencing, revealed presence of a T790M mutation (data not shown). Tumor shrinkage on

AZD9291 was 39.7% at scan 1, 48.3% by scan 2 **(Fig. 7B)**, remained at 48.3% at both scan 3 and scan 4, and was 51.7% at scan 5 (data not shown).

The second patient was a 57-year old white female never smoker from England diagnosed with Stage IV lung adenocarcinoma in December 2010. Analysis of tumor tissue obtained at diagnosis in a local molecular pathology lab using the Qiagen EGFR RGQ PCR test revealed evidence of exon 19 deletion and T790M mutations (data not shown). The patient was treated with first-line gefitinib, achieving a partial response before eventual progressive disease 14 months later, suggesting that the T790M mutation was present at only a low allele frequency. Re-biopsy prior to starting AZD9291 was not performed. At the cycle 1 day 15 assessments on AZD9291, the patient reported full resolution of pre-existing persistent nocturnal cough. Tumor shrinkage was 38% at scan 1, 39.3% at scan 2, 56.7% by scan 3 **(Fig. 7C)**, 62% by scan 4, and 59.3% by scan 5 (data not shown). By Cycle 7 Day 1, the patient reported significant improvement in pre-existing hair and eyelash abnormalities which had developed during the immediately prior gefitinib therapy. Since this patient received AZD9291 after developing acquired resistance whilst on continuous gefitinib (after initial > 6 months duration of partial response) with no intervening treatment, strict Jackman clinical criteria for acquired resistance were fulfilled (50). No significant aberration of blood glucose levels were noted in either patient during the study. Both patients had a duration of response of approximately 9 months and were progression-free on 20 mg/day AZD9291 for approximately 11 months, until disease progression by RECIST 1.1. Both patients continue to receive AZD9291 treatment on study as per protocol, as they continue to derive clinical benefit according to their treating physicians.

Discussion

Mutations in EGFR occur in 10-35% of NSCLCs and confer sensitivity to the EGFR TKIs erlotinib, gefitinib, and afatinib (6). In randomized studies, the median overall survival of patients with EGFR mutant lung cancer receiving first-line EGFR TKIs is ~19-36 months, while median progression free survival is about a year. In more than half of patients, tumor cells at the time of progression harbor a second-site T790M mutation, which confers resistance to these EGFR TKIs (23). No specific treatments for patients with acquired resistance to current EGFR TKIs have yet been approved.

We describe here the identification, characterization and early clinical development of AZD9291, a novel oral, irreversible, third generation TKI with a distinct profile from gefitinib, erlotinib, afatinib, and dacomitinib. Notably, AZD9291 has a distinct chemical structure from the other third-generation TKIs, WZ4002 (34) and CO-1686 (51). Biochemical profiling together with *in vitro* cellular phosphorylation and phenotype studies have collectively shown that AZD9291 is highly potent against EGFRm+ and T790M resistant EGFR mutants with a wide margin of selectivity against wild type EGFR activity and exhibits a high degree of selectivity against other kinases outside the EGFR family. Moreover, the profound anti-tumor activity of AZD9291 across xenograft and transgenic mutant T790M EGFR disease models *in vivo* suggests the potential to target T790M tumors following progression on early generation TKIs.

Prior to identification of "third generation" EGFR TKIs, the most promising targeted regimen in patients with acquired resistance had been the combination of afatinib plus cetuximab, which induced a 32% response rate and median progression-free survival of 4.7 months in a heavily pre-treated cohort (52) with a significant degree of skin and gastrointestinal (diarrhea) toxicity. In the phase I trial of AZD9291 in EGFRm+ NSCLC patients that had progressed on earlier generation TKIs, evidence of efficacy has been seen at all doses studied so far, with AZD9291 induced partial radiographic responses in patients whose tumors were known to harbor T790M, from the first dose cohort onwards (49, 53). Rash and diarrhea were mostly mild and reported in only a minority of patients, consistent with low activity against wild-type EGFR. Out of the two confirmed partial responses described in this paper, in addition to both patients' tumors harboring the T790M mutations (according to local tests), one patient's disease fits strict Jackman criteria for acquired resistance (50), receiving the drug directly after prolonged response and progression on gefitinib. Thus, based on the above, AZD9291 has already demonstrated proof-of-principle clinical activity in patients with acquired resistance for whom there are no approved targeted therapies. Similarly, results from a phase I trial with CO-1686 have also shown evidence of efficacy in TKI-resistant tumors harboring T790M (54) (55), providing further proof of principle for potential use of "third generation" TKIs in this setting. A surprising finding in the afatinib plus cetuximab study was that tumors with undetectable levels of T790M also displayed tumor shrinkage, suggesting that a T790M-independent but EGFR-dependent pathway of resistance exists. The current phase I study of AZD9291 will test whether the drug is effective in both T790M-positive and –negative cohorts, through planned dose-expansion cohorts. Full Phase I data will be presented at completion of study.

The existence of cell populations harboring T790M within a proportion of TKI-naïve EGFRm+ tumors has been reported, although the prevalence depends on the diagnostic assay being used. Studies using more conventional diagnostic assays have reported detection in about 2% of TKI-naïve tumors (56). Recently, groups using more sensitive technologies have reported higher detection rates ranging from 40% to 60% (57), although it remains unclear whether all these observations are real or analytical artifacts (58). However, overall the data supports the hypothesis that T790M clones pre-exist in a proportion of EGFRm+ tumors prior to TKI treatment. In addition to T790M, AZD9291 also potently inhibits sensitizing mutant EGFR across *in vitro* and *in vivo* disease models at similar potencies to T790M-mutant EGFR. Therefore, taken together, this supports the hypothesis that AZD9291 could also offer an attractive treatment option in EGFRm+ TKI-naïve patients, through targeting both sensitizing and T790M tumour cell populations that co-exist in a proportion of tumors, which may then lead to delayed disease progression and ultimately increased survival benefit. However, it remains to be determined what the optimal sequencing of EGFR TKIs will be and whether maximum benefit to most patients will be achieved through using AZD9291 after TKI progression or earlier in the treatment pathway.

Patients harboring EGFRm+ tumors often progress during TKI treatment due to growth of secondary brain metastases (BM) (59). Although there are reports of TKIs providing benefit in treatment of EGFRm+ BM, current TKIs are believed to have generally poor properties for penetrating across the blood brain barrier (BBB), and thus their activity will be variable

and influenced by such factors as dose, level of BBB disruption and efflux transporter expression across individuals. Therefore, there is also a need for EGFR TKIs with improved brain penetrance. Quantitative whole body autoradiography (QWBA) studies in rat brain with [^{14}C]AZD9291 have indicated AZD9291 had a brain-to-blood ratio of up to 2 over the first 24 hours, suggesting the potential of AZD9291 to penetrate the brain (data not shown). This is in contrast to [^{14}C]gefitinib which had a maximum brain-to-blood ratio of only 0.2 (60). Although further pre-clinical studies are required to explore the translatable potential of AZD9291 to target brain metastases, together with future clinical studies, the preliminary data look promising in this area.

Despite the potential of AZD9291 to prevent resistance via T790M, tumors are likely to engage alternative escape mechanisms. If TKIs such as AZD9291 become a prominent feature in the treatment of EGFRm+ disease across multiple lines of therapy, it will be critical for future pre-clinical and clinical research to identify the most prevalent future resistance mechanisms. Consistent with its pharmacological profile, we have not observed acquired resistance to AZD9291 *in vitro* due to emergence of T790M. It is also interesting to note that we not yet seen resistance to AZD9291 due to direct mutation of cysteine 797 (data not shown), which would render the receptor refractory to irreversible agents, in an analogous manner T790M prevents inhibition by early generation drugs. Therefore, non-EGFR related resistance mechanisms may become more dominant for agents such as AZD9291. Indeed, pre-clinical reports have suggested that "third generation" agents can induce switching to multiple signaling mechanisms that bypass EGFR dependency such as ERK and AKT pathways (35, 61, 62). Since AZD9291 is structurally distinct, it will be critical to understand which resistance mechanisms are induced through treatment with AZD9291 and whether different "third generation" TKIs engage common escape mechanisms. Furthermore, identification of molecular mechanisms of resistance will support the investigation of strategies to combine additional novel targeted therapies with AZD9291 as a foundation EGFR TKI partner, to achieve potentially greater clinical benefit.

AZD9291 and its active circulating metabolite AZ5104 display similar and minimal off-target activity against other non-HER family kinases, but *in vitro* data suggests the potential to target both HER2 and HER4 kinase activity. This property may be important as HER2 amplification may mediate acquired resistance to EGFR TKI in some cases (13). AZD9291 and AZ5104 also appear to be effective against other rare drug-sensitive EGFR mutants and potentially lung cancer-associated HER2 mutants, but like other EGFR TKIs are not potent against an EGFR exon 20 insertion. Further pre-clinical and clinical studies are required to understand the potential utility of AZD9291 in these additional molecular phenotypes.

Earlier generation EGFR TKIs have revolutionized the treatment of EGFRm+ NSCLC and have demonstrated the power of precision medicine in genetically-defined tumors. However, toxicities related to wild-type EGFR and the emergence of resistance mechanisms have limited the effectiveness of these drugs. Third generation EGFR TKI agents such as AZD9291 have the potential to overcome these limitations and improve markedly the treatment options to patients who have progressed on TKI treatment due to T790M. Evaluation of AZD9291 in the 1st line setting in patients with EGFRm+tumors should also be considered based on AZD9291's third generation EGFR TKI profile. Moreover, if

AZD9291 is confirmed to have a mild side effect profile together with its clinical efficacy and mechanistic hypothesis, this raises the option for investigation as a foundation EGFR TKI for combinations with other therapies to provide further treatment options for patients.

Materials and Methods

Modelling the binding mode of AZD9291

A published structure of the EGFR T790M mutant (pdb code 3IKA (34)) was used for the modelling of potential binding modes of AZD9291. Crystal structures were prepared using the protein preparation wizard in Maestro (Schrödinger Release 2013-1) which optimises hydrogen placements. The active site was defined by using the bound ligand, and the covalent docking protocol was used to model potential binding modes. These were ranked using the assigned scores and manually inspected for the retention of the key hinge interactions to the hinge region residue M793.

Cell lines—All AZ cell lines were tested and authenticated by short-tandem repeat analysis (STR). PC-9 cells were obtained in Nov 2011 from Akiko Hiraide at Preclinical Sciences R&D AZ Japan and last STR tested in May 2013. NCI-H1975 (H1975; CRL-5908. Obtained 2004 and last STR tested Nov 2012), Calu-3 (HTB-55. Obtained 2010 and last STR tested June 2013), NCI-H1650 (H1650; CRL-5883. Obtained 2004 and last STR tested Sept 2011) and NCI-H2073 (H2073; CRL-5918. Obtained 2007 and last STR tested Nov 2012) cells were obtained from ATCC. LoVo cell line (CCL-229) was obtained from ECACC in 1995 and last STR tested Jan 2013. PC-9 Vandetinib resistant cells (PC-9VanR) were obtained in 2010 from Dr. Kiura at Okayama University and last STR tested Sept 2011. A431 cell line was obtained in 2004 from Prof Mike Waterfield at ICRF London and STR tested May 2012. All other cell lines were available in the Pao lab and have been used as reagents in the Pao Lab since 2005. Pao lab cell lines were re-genotyped multiple times to confirm the presence of known *EGFR* mutations by standard Sanger sequencing to ensure the accuracy of experiments. . Cells were cultured in standard RPMI media (Corning) supplemented with 10% heat-inactivated fetal bovine serum (Atlanta Biologicals), 2mM L-glutamine (Corning) and 1% penicillin/streptomycin (Corning) and grown in a humidified incubator with 5% CO_2 at 37°C. Resistant cells were maintained under constant TKI selection prior to use in experiments.

In vitro **EGFR phosphorylation assays**—Cells were treated for 2 h with a dose-response of each drug. Wild-type cells were stimulated for 10 minutes with 25 ng/ml of EGF before lysis. Level of EGFR phosphorylation was quantified in cell extracts using a modified R&D Systems DuoSet Human phospho-EGFR ELISA (36).

In vitro **cell phenotype assays**—Cellular Sytox proliferation assays were performed as described (36) and Origin software used to interpolate IC_{50} values. Growth inhibition assays were performed using CellTiter Blue Reagent (Promega, G8081) as described, (13) and IC_{50} values were calculated using Excel (Microsoft).

Generation of EGFR inhibitor resistant cell populations—PC-9 cells were seeded into T75 flasks (5×10^5 cells / flask) in RPMI growth media and incubated at 37°C, 5%

CO_2. The following day the media was replaced with media supplemented with a concentration of EGFR inhibitor equal to the EC_{50} concentration predetermined in PC-9 cells. Media changes were carried out every 2-3 days and resistant clones allowed to grow to 80% confluency prior to the cells being trypsinised and reseeded at the original seeding density in media containing twice the concentration of EGFR inhibitor. Dose escalations were continued until a final concentration of 1.5μM gefitinib, 1.5μM afatinib, 1.5μM WZ4002 or 160nM AZD9291 were achieved.

Expression vectors and transfections—The indicated EGFR cDNAs were cloned into the pcDNA3.1(-) expression vector and altered using site-directed mutagenesis as described (5). All cDNAs were re-sequenced to verify that no additional codon-changing mutations were present. pCDH-puro-EGFRvIII lacking exons 2-7 in EGFR (a kind gift from Dr. Jialiang Wang, Vanderbilt University) was constructed by subcloning the EGFRvIII fragment from MSCV-XZ066-EGFRvIII (Addgene Plasmid# 20737 http://www.addgene.org/20737/) into the expression vector pCDH-CMV-MCS-EF1-Puro. pBabe-HER2YVMA-puro (a kind gift from Carlos Arteaga, Vanderbilt University) encodes HER2 with an in-frame YVMA insertion at residue 776 (43). All plasmids were transfected into 293 cells as described (5).

Immunoblotting—Cells were washed on ice with cold PBS before addition of radioimmunoprecipatation assay (RIPA) buffer (150 mmol/L Tris-HCl, pH 7.5, 150 mmol/L NaCl, 1% NP-40 substitute, 0.1% SDS) supplemented with protease inhibitor cocktail (Roche), 40mmol/L sodium fluoride, 1 mmol/L soldium orthovanadate, and 1 μmol/L okadaic acid. After scraping, lysates were transferred to microcentrofuge tubes and shaken at 4°C for 20 minutes before 10 minute centrifugation and protein quantification with Bradford Reagent (Bio-Rad). Equal protein amounts were loaded for SDS-PAGE using 4-12% gradient or 10% Bis-Tris precast gels (Novex Life Technologies), followed by transfer to polyvinylidene difluoride membranes using the iBlot dry transfer system (Novex Life Technologies). After blocking in 5% BSA-TBST or milk-TBST, membranes were blotted with total EGFR (BD Biosciences, #610017), phospho-EGFR (Tyr1068, R&D Systems, MAB3570 or Tyr1173, Santa Cruz Technologies, Inc, sc-12351), total AKT (Cell Signaling, 9272S), phospho-AKT (Ser473, Cell Signaling, 9271L), total ERK (Cell Signaling, 9102L), phospho-ERK (Thr202/Tyr204, Cell Signaling, 9101L), prosurfactant protein C (Abcam, ab90716) or actin (Sigma, A2066) followed by horseradish peroxidase (HRP)-conjugated secondary antibodies (Cell Signaling, 7074 or 7076). Signals were detected with Western Lightening Plus detection reagents (Perkin Elmer, NEL10500NEA).

Molecular genotyping—AZD9291 resistant cells were assessed for EGFR T790M and other recurrent lung-associated mutations using an established assay (63).

Xenograft studies—All studies involving animals in the UK were conducted in accordance with UK Home Office legislation, the Animal Scientific Procedures Act 1986 (ASPA) and with Astrazeneca Global Bioethics policy. All experimental work is outlined in project licence 40/3483 which has gone through the AstraZeneca Ethical Review Process. NCI-H1975 and A431 cells for *in vivo* implant were cultured in DMEM (Invitrogen)

supplemented with 10% v/v fetal calf serum (Sigma Aldrich) and 1% v/v L-glutamine (Invitrogen). PC-9 cells were cultured in RPMI 1640 (Invitrogen) supplemented with 10%v/v fetal calf serum, 1% v/v L-glutamine and 10% v/v M1 supplement (Egg Technologies). All cell lines were then cultured in a humidified incubator with 7.5% CO_2 at 37°C. Cells were detached using 0.05% trypsin (Invitrogen) and re-suspended for implant in serum-free media. 5×10^6 cells were implanted subcutaneously in a total volume of 0.1ml/ mouse for PC-9 and NCI-H1975, and 1×10^7 cells implanted subcutaneously for A431. Both PC-9 and A431 cells were implanted in 50% matrigel. PC-9 xenografts were established in female scid mice and NCI-H1975 and A431 were established in female nude mice. All mice were greater than 6 weeks old at time of cell implant. Tumor growth was monitored twice weekly by bilateral caliper measurements, tumor volume calculated, and mice randomized into vehicle or treatment groups with approximate mean start size of 0.2-0.4cm^3. Randomisation for animal studies is based on initial tumor volumes to ensure equal distribution across groups. A power analysis is performed whereby group sizes are calculated to enable statistically robust detection of tumor growth inhibition. Mice were dosed once daily by oral gavage for duration of the treatment period. Tumor growth inhibition from start of treatment was assessed by comparison of the mean change in tumor volume for the control and treated groups. Statistical significance was evaluated using a one-tailed Students t test.

For pharmacodynamic studies, mice were randomized at a mean tumor volume of approximately 0.5-0.8cm^3 using the same randomization criteria as the tumor growth inhibition studies. Mice were then treated orally with a single bolus dose of either vehicle or AZD9291. Tumors were excised at specific timepoints after dosing and fixed in 10% buffered formalin. Immunohistochemical analysis was performed on formalin fixed, paraffin embedded tissue sections staining for phosphorylated EGFR (Tyr1173) and phosphorylated ERK (p44/42 Thr202/Tyr204).

Transgenic Mouse Studies—All animals were kept in pathogen-free housing under guidelines approved by the Vanderbilt University Medical Center Institutional Animal Care and Use Committee. The generation of EGFR[L858R] (45) and EGFR[L858R+T790M] mice (male and female) was previously described (46) Doxycycline was administered by feeding mice (aprox 3 week old) with doxycycline-impregnated food pellets (625 ppm; Harlan-Teklad), and treated for about 3 months during which time tumors developed. Afatinib and AZD9291 were suspended in 1% Polysorbate 80 and administered via oral gavage once daily at the doses of 7.5 mg/kg and 5 mg/kg, respectively. Mice were imaged weekly at the Vanderbilt University Institute of Imaging Science. For immunoblot analysis, mice were treated for eight hours with drug as described before dissection and flash freezing of the lungs. Lungs were pulverized in liquid nitrogen before lysis as described above.

MRI—All procedures were approved by Vanderbilt's Institutional Animal Care and Usage Committee. Mice were anesthetized via inhalation of 2%/98% isoflurane/oxygen and maintained under anesthesia throughout the course of the experiment. Animals were secured in a prone position in a 38-mm inner diameter radiofrequency (RF) coil and placed in a Varian 7T horizontal bore imaging system (Varian Inc, Palo Alto, CA) for data collection. A

constant body temperature of 37°C was maintained using heated air flow. Prior to treatment, mice were scanned at least twice to confirm the presence of growing lung nodules and to avoid treating false-positive animals.

Multi-slice T1-weighted gradient echo images were collected in all three imaging planes (axial, sagittal, and coronal) for localization of the lungs (repetition time (TR) = 100ms, echo time (TE) = 5ms, slice thickness = 1mm, 40mm × 40mm field of view (FOV), approximately 15-20 slices). Following the initial scout imaging, respiratory triggered, segmented fast low angle shot (FLASH) images were collected in both the axial and coronal planes with TR/TE = 850/2.8ms, flip angle = 15 degrees, number of slices = 22, slice thickness = 0.7mm with a 0.2mm gap between slices, and number of acquisitions = 16. For the axial images, the FOV = 23.04mm × 23.04mm, with a matrix size of 256×256, resulting in an in-plane resolution of 90 microns. For the coronal orientation, FOV = 30.72mm × 23.04mm, with a data matrix = 256×256, resulting in an in-plane resolution of 120×90 microns.

Following image acquisition, lung tumor volume measurements were performed using Matlab 2012a (The MathWorks, Inc, Natick, MA). A region of interest (ROI) was manually drawn around the lungs for each slice, excluding the heart, and a signal intensity threshold of 25 times the noise level (defined as the standard deviation of signal intensities in a region of the image background) was used to segment voxels within that ROI as positive for tumor. Total lung tumor volume was then calculated by multiplying the tumor area within the segmented region by 0.09 cm (the distance between each MRI slice).

Immunohistochemistry

4um sections were deparaffinized with xylene and rehydrated through graded alcohols into water. Antigen retrieval was carried out in a Milestone RHS microwave rapid histoprocessor for 10 minutes at 110°C in pH9 buffer, Dako S2367 (for phospho-EGFR and phospho-Akt) and pH 6 citrate buffer, Dako S1699 (for phospho-Erk and phospho-S6). Tissues were placed on a LabVision Autostainer, endogenous peroxidase was blocked with 3% H_2O_2 for 10 minutes, followed by washing twice in TBS/0.05% Tween. Serum free protein block (Dako; X0909) was applied for 15 minutes. Slides were then incubated with the primary antibodies at room temperature, phospho-EGFR Tyr1173 (Cell Signaling Technology, code 4407) at a 1:200 dilution, phospho-ERK (p44/42 Thr202/Tyr204) (Cell Signaling Technology, code 4376) at 1:100, phospho-S6 (Ser 235/236) CST #4857 at 1:150, phospho-PRAS40 (pThr246) (Cell Signaling Technology, code #2997) at 1:200, and phospho-Akt308 CST #2965 at 1:100 dilution. After washing twice, sections were incubated for 30 minutes with Rabbit Envision polymer detection system (Dako K4003), washed twice and then developed in liquid 3,3_-diaminobenzidine (DAB) for 10 minutes. Sections were then counter-stained with Mayer's haematoxylin, dehydrated, cleared, and mounted with coverslips.

Patients—All patients were treated on trial NCT01802632 with written informed consent from patients and approval appropriate Institutional Review Boards (For the two patients disclosed in this manuscript the Ethics committees are as follows; Korean patient: Seoul

National University Hospital (EC), UK patient: North West – GM Central, North West Centre of REC, Manchester). Consent to publish study CT scan images is included as part of the patient informed consent, signed by both patients. In the first into man study a cohort size of 6 for the starting dose is standard practice, to provide sufficient safety and tolerability data about a dose level without exposing too many patients to a dose which may not be clinically beneficial. The first two patients in the starting dose cohort with an objective response were selected for inclusion in the publication. The clinical study is ongoing and further study data will be submitted for publication at a later date.

Patient tumor genotyping in the trial—Patient tumor tissues were analyzed for EGFR mutations using either the Qiagen EGFR RGQ PCR Kit [Cat #870111] or direct dideoxynucleotide sequencing.

Supplementary Material

Refer to Web version on PubMed Central for supplementary material.

Acknowledgements

Abbreviations

EGF	epidermal growth factor
EGFR	EGF receptor
EGFRm+	EGFR mutant NSCLC tumors
EMT	epithelial mesenchymal transition
IGF-1R	insulin-like growth factor receptor
IR	insulin receptor
NSCLC	Non small cell lung cancer
TKI	tyrosine kinase inhibitor

Literature Cited

1. Barker AJ, Gibson KH, Grundy W, Godfrey AA, Barlow JJ, Healy MP, et al. Studies leading to the identification of ZD1839 (IRESSA): an orally active, selective epidermal growth factor receptor tyrosine kinase inhibitor targeted to the treatment of cancer. Bioorg Med Chem Lett. 2001; 11:1911–4. [PubMed: 11459659]

2. Moyer JD, Barbacci EG, Iwata KK, Arnold L, Boman B, Cunningham A, et al. Induction of apoptosis and cell cycle arrest by CP-358,774, an inhibitor of epidermal growth factor receptor tyrosine kinase. Cancer Research. 1997; 57:4838–48. [PubMed: 9354447]

3. Lynch TJ, Bell DW, Sordella R, Gurubhagavatula S, Okimoto RA, Brannigan BW, et al. Activating mutations in the epidermal growth factor receptor underlying responsiveness of non-small-cell lung cancer to gefitinib. The New England Journal of Medicine. 2004; 350:2129–39. [PubMed: 15118073]

4. Paez JG, Janne PA, Lee JC, Tracy S, Greulich H, Gabriel S, et al. *EGFR* mutations in lung cancer: correlation with clinical response to gefitinib therapy. Science. 2004; 304:1497–500. [PubMed: 15118125]

5. Pao W, Miller V, Zakowski M, Doherty J, Politi K, Sarkaria I, et al. EGF receptor gene mutations are common in lung cancers from "never smokers" and are associated with sensitivity of tumors to gefitinib and erlotinib. Proceedings of the National Academy of Sciences of the United States of America. 2004; 101:13306–11. [PubMed: 15329413]

6. Pao W, Chmielecki J. Rational, biologically based treatment of EGFR-mutant non-small-cell lung cancer. Nature Reviews Cancer. 2010; 10:760–74.

7. Maemondo M, Inoue A, Kobayashi K, Sugawara S, Oizumi S, Isobe H, et al. Gefitinib or chemotherapy for non-small-cell lung cancer with mutated EGFR. The New England Journal of Medicine. 2010; 362:2380–8. [PubMed: 20573926]

8. Mitsudomi T, Morita S, Yatabe Y, Negoro S, Okamoto I, Tsurutani J, et al. Gefitinib versus cisplatin plus docetaxel in patients with non-small-cell lung cancer harbouring mutations of the epidermal growth factor receptor (WJTOG3405): an open label, randomised phase 3 trial. The Lancet Oncology. 2009; 11:121–8. [PubMed: 20022809]

9. Mok TS, Wu YL, Thongprasert S, Yang CH, Chu DT, Saijo N, et al. Gefitinib or carboplatin-paclitaxel in pulmonary adenocarcinoma. The New England Journal of Medicine. 2009; 361:947–57. [PubMed: 19692680]

10. Rosell R, Carcereny E, Gervais R, Vergnenegre A, Massuti B, Felip E, et al. Erlotinib versus standard chemotherapy as first-line treatment for European patients with advanced EGFR mutation-positive non-small-cell lung cancer (EURTAC): a multicentre, open-label, randomised phase 3 trial. The Lancet Oncology. 2012; 13:239–46. [PubMed: 22285168]

11. Zhou C, Wu YL, Chen G, Feng J, Liu XQ, Wang C, et al. Erlotinib versus chemotherapy as first-line treatment for patients with advanced EGFR mutation-positive non-small-cell lung cancer (OPTIMAL, CTONG-0802): a multicentre, open-label, randomised, phase 3 study. The Lancet Oncology. 2011; 12:735–42. [PubMed: 21783417]

12. Burtness, B.; Anadkat, M.; Basti, S.; Hughes, M.; Lacouture, ME.; McClure, JS., et al. Journal of the National Comprehensive Cancer Network : JNCCN. Vol. 7. Suppl 1: 2009. NCCN Task Force Report: Management of dermatologic and other toxicities associated with EGFR inhibition in patients with cancer.; p. S5-21.quiz S2-4

13. Takezawa K, Pirazzoli V, Arcila ME, Nebhan CA, Song X, de Stanchina E, et al. HER2 Amplification: A Potential Mechanism of Acquired Resistance to EGFR Inhibition in EGFR-Mutant Lung Cancers That Lack the Second-Site EGFRT790M Mutation. Cancer Discovery. 2012; 2:922–33. [PubMed: 22956644]

14. Bean J, Brennan C, Shih JY, Riely G, Viale A, Wang L, et al. MET amplification occurs with or without T790M mutations in EGFR mutant lung tumors with acquired resistance to gefitinib or erlotinib. Proceedings of the National Academy of Sciences of the United States of America. 2007; 104:20932–7. [PubMed: 18093943]

15. Engelman JA, Zejnullahu K, Mitsudomi T, Song Y, Hyland C, Park JO, et al. MET amplification leads to gefitinib resistance in lung cancer by activating ERBB3 signaling. Science. 2007; 316:1039–43. [PubMed: 17463250]

16. Sequist LV, Waltman BA, Dias-Santagata D, Digumarthy S, Turke AB, Fidias P, et al. Genotypic and histological evolution of lung cancers acquiring resistance to EGFR inhibitors. Science Translational Medicine. 2011; 3:75ra26.

17. Ohashi K, Sequist LV, Arcila ME, Moran T, Chmielecki J, Lin YL, et al. Lung cancers with acquired resistance to EGFR inhibitors occasionally harbor BRAF gene mutations but lack mutations in KRAS, NRAS, or MEK1. Proceedings of the National Academy of Sciences of the United States of America. 2012; 109:E2127–33. [PubMed: 22773810]

18. de Bruin EC, Cowell CF, Warne PH, Jiang M, Saunders RE, Melnick MA, et al. Reduced NF1 expression confers resistance to EGFR inhibition in lung cancer. Cancer Discovery. 2014; 4:606–619. [PubMed: 24535670]

19. Ware KE, Marshall ME, Heasley LR, Marek L, Hinz TK, Hercule P, et al. Rapidly acquired resistance to EGFR tyrosine kinase inhibitors in NSCLC cell lines through de-repression of FGFR2 and FGFR3 expression. PloS one. 2010; 5:e14117. [PubMed: 21152424]

20. Kobayashi S, Boggon TJ, Dayaram T, Janne PA, Kocher O, Meyerson M, et al. *EGFR* mutation and resistance of non-small-cell lung cancer to gefitinib. New England Journal of Medicine. 2005; 352:786–92. [PubMed: 15728811]

21. Pao W, Miller VA, Politi KA, Riely GJ, Somwar R, Zakowski MF, et al. Acquired resistance of lung adenocarcinomas to gefitinib or erlotinib is associated with a second mutation in the EGFR kinase domain. PLoS Medicine. 2005; 2:e73. [PubMed: 15737014]

22. Sos ML, Rode HB, Heynck S, Peifer M, Fischer F, Kluter S, et al. Chemogenomic profiling provides insights into the limited activity of irreversible EGFR Inhibitors in tumor cells expressing the T790M EGFR resistance mutation. Cancer Research. 2010; 70:868–74. [PubMed: 20103621]

23. Yun CH, Mengwasser KE, Toms AV, Woo MS, Greulich H, Wong KK, et al. The T790M mutation in EGFR kinase causes drug resistance by increasing the affinity for ATP. Proceedings of the National Academy of Sciences of the United States of America. 2008; 105:2070–5. [PubMed: 18227510]

24. Li D, Ambrogio L, Shimamura T, Kubo S, Takahashi M, Chirieac LR, et al. BIBW2992, an irreversible EGFR/HER2 inhibitor highly effective in preclinical lung cancer models. Oncogene. 2008; 27:4702–11. [PubMed: 18408761]

25. Engelman JA, Zejnullahu K, Gale CM, Lifshits E, Gonzales AJ, Shimamura T, et al. PF00299804, an irreversible pan-ERBB inhibitor, is effective in lung cancer models with EGFR and ERBB2 mutations that are resistant to gefitinib. Cancer Research. 2007; 67:11924–32. [PubMed: 18089823]

26. Ramalingam SS, Blackhall F, Krzakowski M, Barrios CH, Park K, Bover I, et al. Randomized phase II study of dacomitinib (PF-00299804), an irreversible pan-human epidermal growth factor receptor inhibitor, versus erlotinib in patients with advanced non-small-cell lung cancer. J Clin Oncol. 2012; 30:3337–44. [PubMed: 22753918]

27. Sequist LV, Yang JC, Yamamoto N, O'Byrne K, Hirsh V, Mok T, et al. Phase III Study of Afatinib or Cisplatin Plus Pemetrexed in Patients With Metastatic Lung Adenocarcinoma With EGFR Mutations. J Clin Oncol. 2013; 31:3327–3334. [PubMed: 23816960]

28. Miller VA, Hirsh V, Cadranel J, Chen YM, Park K, Kim SW, et al. Afatinib versus placebo for patients with advanced, metastatic non-small-cell lung cancer after failure of erlotinib, gefitinib, or both, and one or two lines of chemotherapy (LUX-Lung 1): a phase 2b/3 randomised trial. The Lancet Oncology. 2012; 13:528–38. [PubMed: 22452896]

29. Katakami N, Atagi S, Goto K, Hida T, Horai T, Inoue A, et al. LUX-Lung 4: A Phase II Trial of Afatinib in Patients With Advanced Non-Small-Cell Lung Cancer Who Progressed During Prior Treatment With Erlotinib, Gefitinib, or Both. J Clin Oncol. 2013; 31:3335–3341. [PubMed: 23816963]

30. Eskens FA, Mom CH, Planting AS, Gietema JA, Amelsberg A, Huisman H, et al. A phase I dose escalation study of BIBW 2992, an irreversible dual inhibitor of epidermal growth factor receptor 1 (EGFR) and 2 (HER2) tyrosine kinase in a 2-week on, 2-week off schedule in patients with advanced solid tumours. British Journal of Cancer. 2008; 98:80–5. [PubMed: 18026190]

31. Chmielecki J, Foo J, Oxnard GR, Hutchinson K, Ohashi K, Somwar R, et al. Optimization of dosing for EGFR-mutant non-small cell lung cancer with evolutionary cancer modeling. Science Translational Medicine. 2011; 3:90ra59.

32. Kim Y, Ko J, Cui Z, Abolhoda A, Ahn JS, Ou SH, et al. The EGFR T790M mutation in acquired resistance to an irreversible second-generation EGFR inhibitor. Molecular Cancer Therapeutics. 2012; 11:784–91. [PubMed: 22228822]

33. Janjigian YY, Groen HJM, Horn L, Smit EF, Fu Y, Wang F, et al. Activity and tolerability of afatinib (BIBW 2992) and cetuximab in NSCLC patients with acquired resistance to erlotinib or gefitinib. J Clin Oncol. 2011; 29(suppl) abstr 7525.

34. Zhou W, Ercan D, Chen L, Yun CH, Li D, Capelletti M, et al. Novel mutant-selective EGFR kinase inhibitors against EGFR T790M. Nature. 2009; 462:1070–4. [PubMed: 20033049]

35. Walter AO, Sjin RT, Haringsma HJ, Ohashi K, Sun J, Lee K, et al. Discovery of a mutant-selective covalent inhibitor of EGFR that overcomes T790M-mediated resistance in NSCLC. Cancer Discovery. 2013; 3:1404–15. [PubMed: 24065731]

36. Ward RA, Anderton MJ, Ashton S, Bethel PA, Box M, Butterworth S, et al. Structure- and Reactivity-Based Development of Covalent Inhibitors of the Activating and Gatekeeper Mutant Forms of the Epidermal Growth Factor Receptor (EGFR). Journal of Medicinal Chemistry. 2013; 56:7025–7048. [PubMed: 23930994]

37. Red Brewer M, Yun C-H, Lai D, Lemmon MA, Eck MJ, Pao W. Mechanism for activation of mutated epidermal growth factor receptors in lung cancer. Proceedings of the National Academy of Sciences of the United States of America. 2013; 110:E3595–E3604. [PubMed: 24019492]

38. Sos ML, Koker M, Weir BA, Heynck S, Rabinovsky R, Zander T, et al. PTEN loss contributes to erlotinib resistance in EGFR-mutant lung cancer by activation of Akt and EGFR. Cancer Research. 2009; 69:3256–61. [PubMed: 19351834]

39. Chmielecki J, Pietanza MC, Aftab D, Shen R, Zhao Z, Chen X, et al. EGFR-mutant lung adenocarcinomas treated first-line with the novel EGFR inhibitor, XL647, can subsequently retain moderate sensitivity to erlotinib. J Thoracic Oncol. 2012; 7:434–42.

40. Hickinson DM, Klinowska T, Speake G, Vincent J, Trigwell C, Anderton J, et al. AZD8931, an equipotent, reversible inhibitor of signaling by epidermal growth factor receptor, ERBB2 (HER2), and ERBB3: a unique agent for simultaneous ERBB receptor blockade in cancer. Clinical Cancer Research. 2010; 16:1159–69. [PubMed: 20145185]

41. Wong AJ, Ruppert JM, Bigner SH, Grzeschik CH, Humphrey PA, Bigner DS, et al. Structural alterations of the epidermal growth factor receptor gene in human gliomas. Proc Natl Acad Sci USA. 1992; 89:2965–9. [PubMed: 1557402]

42. Shigematsu H, Takahashi T, Nomura M, Majmudar K, Suzuki M, Lee H, et al. Somatic mutations of the *HER2* kinase domain in lung adenocarcinomas. Cancer Research. 2005; 65:1642–6. [PubMed: 15753357]

43. Wang SE, Narasanna A, Perez-Torres M, Xiang B, Wu FY, Yang S, et al. HER2 kinase domain mutation results in constitutive phosphorylation and activation of HER2 and EGFR and resistance to EGFR tyrosine kinase inhibitors. Cancer Cell. 2006; 10:25–38. [PubMed: 16843263]

44. Merlino GT, Xu YH, Ishii S, Clark AJ, Semba K, Toyoshima K, et al. Amplification and enhanced expression of the epidermal growth factor receptor gene in A431 human carcinoma cells. Science. 1984; 224:417–9. [PubMed: 6200934]

45. Politi K, Zakowski MF, Fan PD, Schonfeld EA, Pao W, Varmus HE. Lung adenocarcinomas induced in mice by mutant EGF receptors found in human lung cancers respond to a tyrosine kinase inhibitor or to down-regulation of the receptors. Genes & Development. 2006; 20:1496–510. [PubMed: 16705038]

46. Regales L, Balak MN, Gong Y, Politi K, Sawai A, Le C, et al. Development of new mouse lung tumor models expressing EGFR T790M mutants associated with clinical resistance to kinase inhibitors. PloS one. 2007; 2:e810. [PubMed: 17726540]

47. Regales L, Gong Y, Shen R, de Stanchina E, Vivanco I, Goel A, et al. Dual targeting of EGFR can overcome a major drug resistance mutation in mouse models of EGFR mutant lung cancer. J Clin Invest. 2009; 119:3000–10. [PubMed: 19759520]

48. Eisenhauer EA, Therasse P, Bogaerts J, Schwartz LH, Sargent D, Ford R, et al. New response evaluation criteria in solid tumours: revised RECIST guideline (version 1.1). Eur J Cancer. 2009; 45:228–47. [PubMed: 19097774]

49. Ranson M, Pao W, Kim D-W, Kim S-W, Ohe Y, Felip E, et al. Preliminary results from a Phase I study with AZD9291: an irreversible inhibitor of epidermal growth factor receptor (EGFR) activating and resistance mutations in non-small cell lung cancer (NSCLC). Eur J Cancer. 2013; 49(suppl 3):S15. abstr LBA33.

50. Jackman D, Pao W, Riely GJ, Engelman JA, Kris MG, Janne PA, et al. Clinical definition of acquired resistance to epidermal growth factor receptor tyrosine kinase inhibitors in non-small-cell lung cancer. J Clin Oncol. 2010; 28:357–60. [PubMed: 19949011]

51. Walter AO, Tjin Tham Sjin R, Haringsma HJ, Ohashi K, Sun J, Lee K, et al. Discovery of a mutant-selective covalent inhibitor of EGFR that overcomes T790M-mediated resistance in NSCLC. Cancer Discovery. 2013; 3:1404–1415. [PubMed: 24065731]

52. Janjigian YY, Smit EF, Horn L, Groen HJM, Camidge DR, Gettinger S, et al. Activity of afatinib/cetuximab in patients with EGFR mutant non-small cell lung cancer and acquired resistance to EGFR inhibitors. Annals of Oncology. 2012; 23(Suppl 9):401. abstr 1227O. [PubMed: 21515665]

53. Ranson M, Pao W, Kim D-W, Kim S-W, Ohe Y, Felip E, et al. AZD9291: an irreversible, potent and selective tyrosine kinase inhibitor (TKI) of activating (EGFRm+) and resistance (T790M) mutations in advanced NSCLC. J Thoracic Oncol. 2013; 8(Suppl 2):S389. abstract MO21.12.

54. Sequist LV, Soria JC, Gadgeel SM, Wakelee HA, Camidge DR, Varga A, et al. First-in-human evaluation of CO-1686, an irreversible, selective, and potent tyrosine kinase inhibitor of EGFR T790M. J Clin Oncol. 2013; 31(suppl) abstr 2524.

55. Soria JC, L.V. S, Gadgeel S, Goldman J, Wakelee H, Varga A, et al. First-in-human evaluation of CO-1686, an irreversible, highly selective tyrosine kinase inhibitor of mutations of EGFR (activating and T790M). J Thoracic Oncol. 2013; 8(Suppl 2):S141. abstr O03.06.

56. Sequist LV, Martins RG, Spigel D, Grunberg SM, Spira A, Janne PA, et al. First-line gefitinib in patients with advanced non-small-cell lung cancer harboring somatic EGFR mutations. J Clin Oncol. 2008; 26:2442–9. [PubMed: 18458038]

57. Costa C, Molina-Vila MA, Drozdowskyj A, Gimenez-Capitan A, Bertran-Alamillo J, Karachaliou N, et al. The impact of EGFR T790M mutations and BIM mRNA expression on outcome in patients with EGFR-mutant NSCLC treated with erlotinib or chemotherapy in the randomized phase III EURTAC trial. Clinical Cancer Research. 2014; 20:2001–2010. [PubMed: 24493829]

58. Ye X, Zhu ZZ, Zhong L, Lu Y, Sun Y, Yin X, et al. High T790M detection rate in TKI-naive NSCLC with EGFR sensitive mutation: truth or artifact? J Thoracic Oncol. 2013; 8:1118–20.

59. Porta R, Sanchez-Torres JM, Paz-Ares L, Massuti B, Reguart N, Mayo C, et al. Brain metastases from lung cancer responding to erlotinib: the importance of EGFR mutation. The European Respiratory Journal. 2011; 37:624–31. [PubMed: 20595147]

60. McKillop D, Hutchison M, Partridge EA, Bushby N, Cooper CMF, Clarkson-Jones JA, et al. Metabolic disposition of gefitinib, an epidermal growth factor receptor tyrosine kinase inhibitor, in rat, dog and man. Xenobiotica. 2004; 34:917–34. [PubMed: 15764411]

61. Cortot AB, Repellin CE, Shimamura T, Capelletti M, Zejnullahu K, Ercan D, et al. Resistance to irreversible EGF receptor tyrosine kinase inhibitors through a multistep mechanism involving the IGF1R pathway. Cancer Research. 2013; 73:834–43. [PubMed: 23172312]

62. Ercan D, Xu C, Yanagita M, Monast CS, Pratilas CA, Montero J, et al. Reactivation of ERK Signaling Causes Resistance to EGFR Kinase Inhibitors. Cancer Discovery. 2012; 2:934–47. [PubMed: 22961667]

63. Su Z, Dias-Santagata D, Duke M, Hutchinson K, Lin YL, Borger DR, et al. A platform for rapid detection of multiple oncogenic mutations with relevance to targeted therapy in non-small-cell lung cancer. The J. Molecular Diagnostics. 2011; 13:74–84.

SIGNIFICANCE

We report development of a novel structurally distinct third generation EGFR TKI, AZD9291, that irreversibly and selectively targets both sensitizing and resistant-T790M mutant EGFR whilst harboring less activity towards wild-type EGFR. AZD9291 is showing promising responses in a Phase I trial even at the first dose level, with first published clinical proof of principle validation being presented.

A
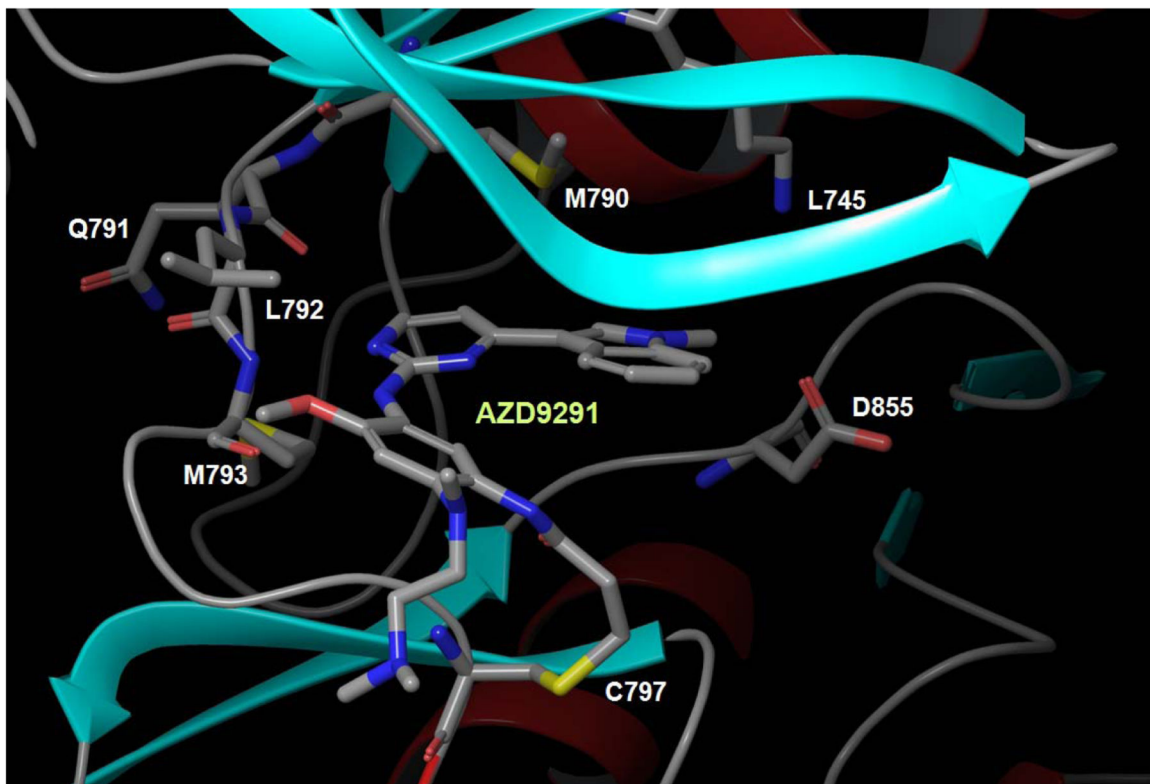
B
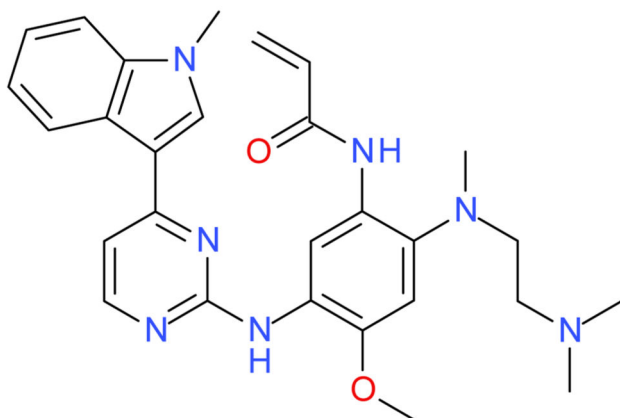
Figure 1.
AZD9291 binding mode and structure. **A,** Structural model showing the covalent mode of binding of AZD9291 to EGFR T790M via Cys-797. Shows pyrimidine core forming two hydrogen bonds to the hinge region (Met-793), orientation of the indole group adjacent to the gatekeeper residue, the amine moiety positioned in the solvent channel and the covalent bond formed to Cys-797 via the acrylamide group of AZD9291. **B,** Chemical structure of AZD9291.

A

	H1975 (L858R/ T790M)	PC-9 VanR (ex19del/ T790M)	PC-9 (ex19del)	H3255 (L858R)	H1650 (ex19del)	LoVo (WT)	A431 (WT)	NCI-H2073 (WT)
AZD9291	15 (10, 20)	6 (3, 13)	17 (13, 22)	60, 49	14, 12	480 (320, 720)	2376, 1193	1865 (872, 3988)
Dacomitinib	40 (24, 65)	6 (2, 17)	0.7 (0.5, 1)	1.2, 1.3	0.04, 0.06	12 (8, 17)	51, 22	26 (7, 99)
Afatinib	22 (15, 31)	3 (2, 6)	0.6 (0.5, 0.8)	1, 0.8	0.6, 3	15 (10, 24)	27, 40	25 (5, 129)
Gefitinib	3102 (1603, 6001)	741 (484, 1136)	7 (5, 11)	11, 12	16, 19	59 (42, 82)	60, 88	61 (34, 110)
Erlotinib	6073 (3634, 10150)	1262 (588, 2711)	6 (4, 7)	8, 11	5, 8	91 (53, 156)	244, 260	108 (52, 223)

B
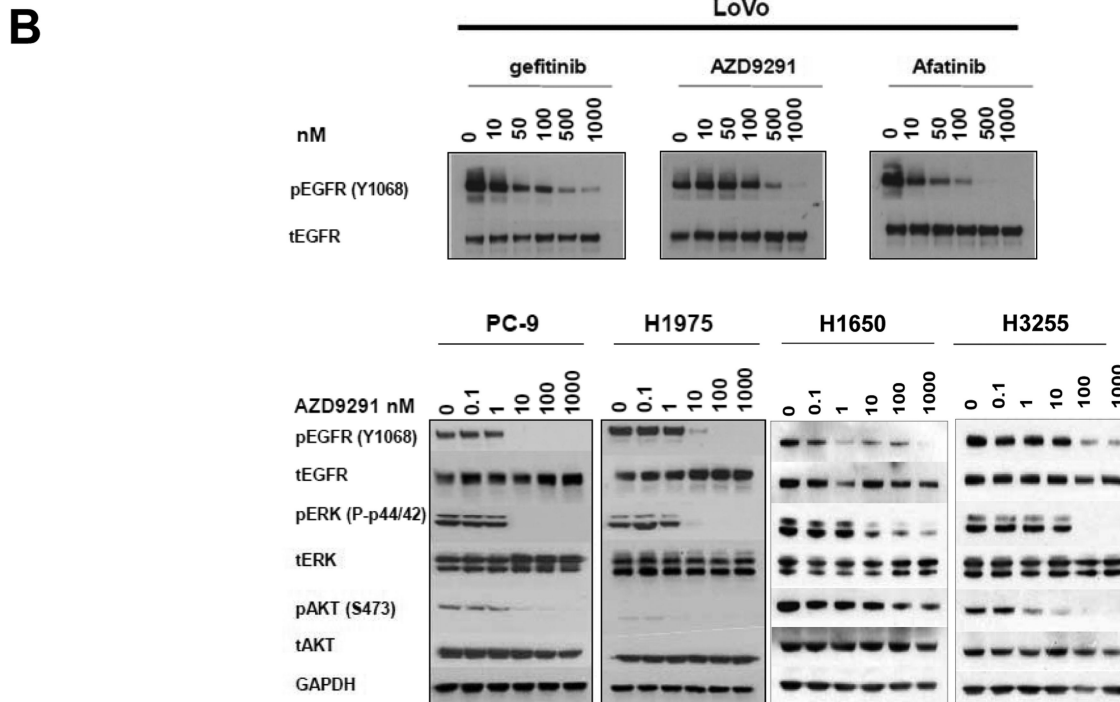
Figure 2.

Effect of AZD9291 on EGFR phosphorylation *in vitro*. **A,** In comparison to early generation TKIs, AZD9291 inhibits EGFR phosphorylation across cell lines harboring sensitising (PC-9, H3255, H1650) or T790M resistance (H1975, PC-9VanR) mutations, whilst having less activity against wild-type EGFR phosphorylation (LOVO, A431, H2073). Apparent geomean IC_{50} (nM) values quantified in cell extracts after 2 h compound treatment using a phospho-EGFR ELISA from at least two separate experiments (expressed with 95% confidence intervals where n>3, or individual IC_{50} values where n=2). **B,** AZD9291 inhibits

EGFR phosphorylation and downstream signaling pathways across representative mutant EGFR lines (PC-9, H1975, H1650, H3255), whilst having less activity against EGFR phosphorylation in the LOVO wild-type EGFR cell line compared to early generation TKIs, after 6 h treatment. The data is representative of at least two separate experiments.

A

|	H1975 (T790M/L858R)	PC-9 VanR (ex19del/T790M)	PC-9 (ex19del)	Calu 3 (WT)	NCI-H2073 (WT)
AZD9291	11 (6,19)	40 (30, 54)	8 (7, 9)	650 (457, 924)	461 (230, 924)
Dacomitinib	335 (265, 424)	531 (465, 607)	0.4 (0.3, 1)	65 (37, 116)	54 (ND)
Afatinib	483 (403, 579)	679 (532, 868)	0.8 (0.7, 0.9)	71 (35, 144)	30 (9, 99)
Gefitinib	6962 (6304, 7688)	4232 (1998, 8965)	23 (20, 25)	1933 (1299, 2876)	200 (41, 974)
Erlotinib	6165 (5392, 7050)	5778 (4766, 7029)	28 (22, 36)	4101 (2732, 6156)	692 (193, 2478)

B
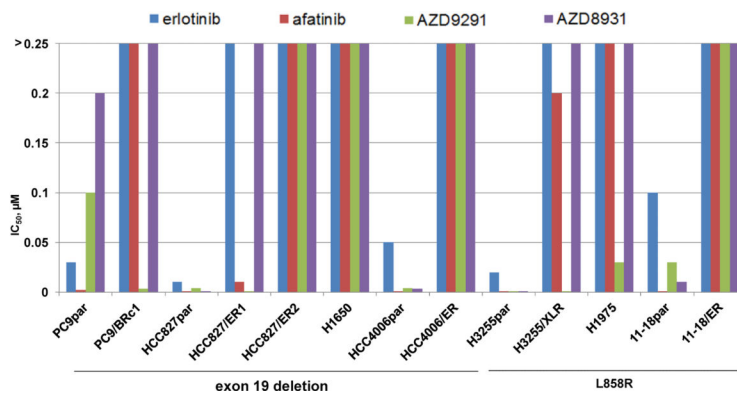
C
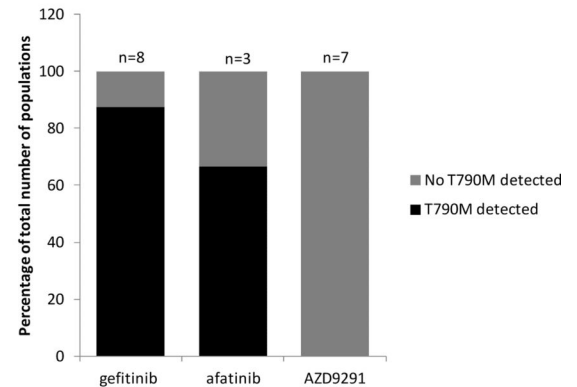
Figure 3.

Additional characteristics of AZD9291 *in vitro*. **A,** AZD9291 demonstrates greater inhibition of viability against mutant EGFR cell lines compared to wild-type, as assessed using a Sytox Green live/dead assay measured after 3 days treatment. The data represents the geomean IC_{50} nM value from at least two separate experiments (expressed with 95% confidence intervals where n>3). **B,** Sensitivity of isogenic pairs of EGFR mutant drug-sensitive and –resistant lung cancer cell lines (PC-9, ex19del; PC-9/BRc1, ex19del/T790M; HCC827, ex19del; HCC827/ER1, ex19del/T790M; HCC827/ER2, ex19del/ METamplification; H1650, ex19del/PTEN loss; HCC4006, ex19del; HCC4006/ER, EMT (epithelial mesenchymal transition); H3255, L858R; H3255/XLR, L858R/T790M; H1975, L858R/T790M; 11-18, L858R; 11-18/ER, L858R/NRAS) to AZD9291, erlotinib, and afatinib. IC_{50}s (μM) were based on data obtained from growth inhibition assays. **C,** T790M mutation was detected in multiple independent populations of PC-9 cells with acquired resistance to gefitinib or afatinib, but not in populations resistant to AZD9291.
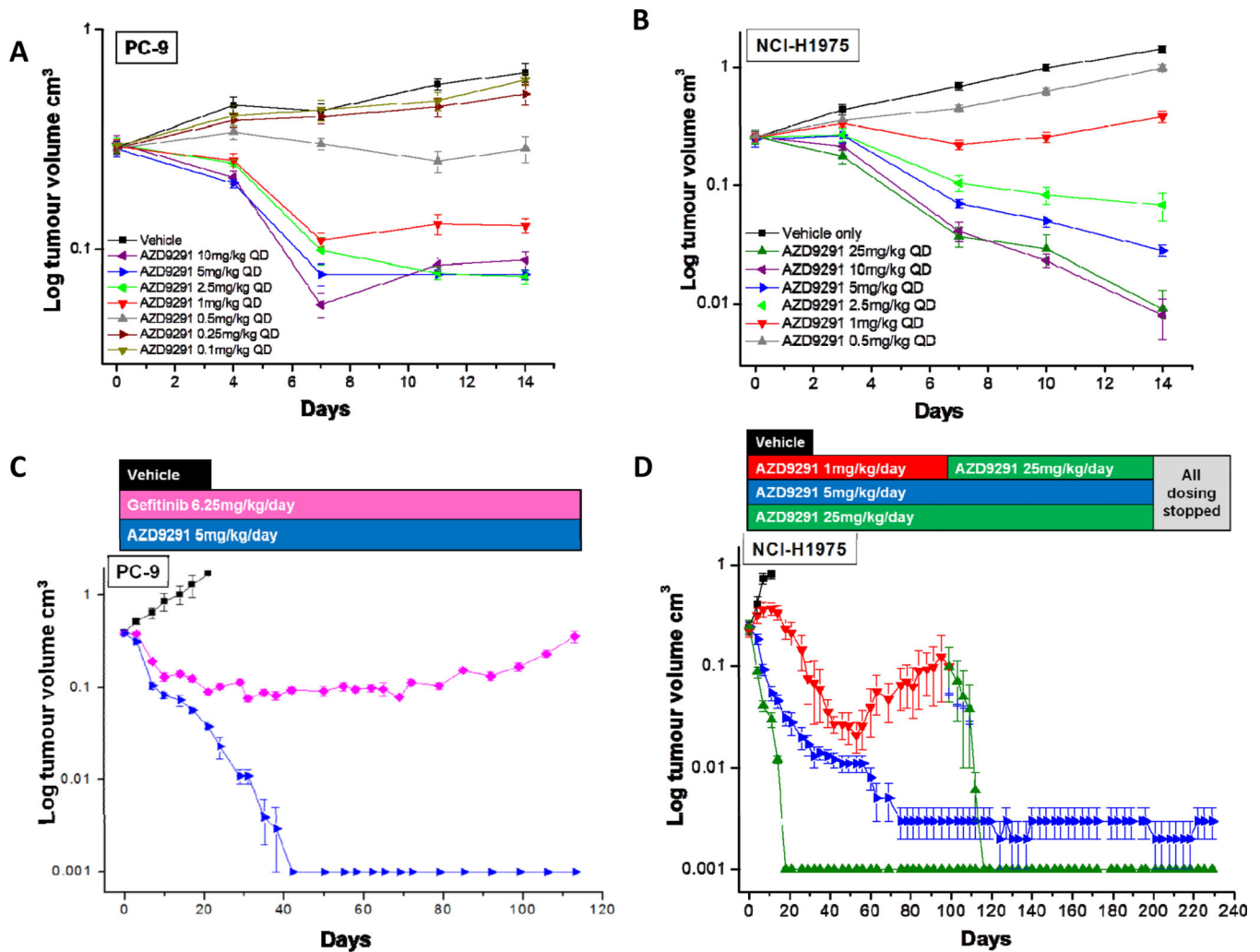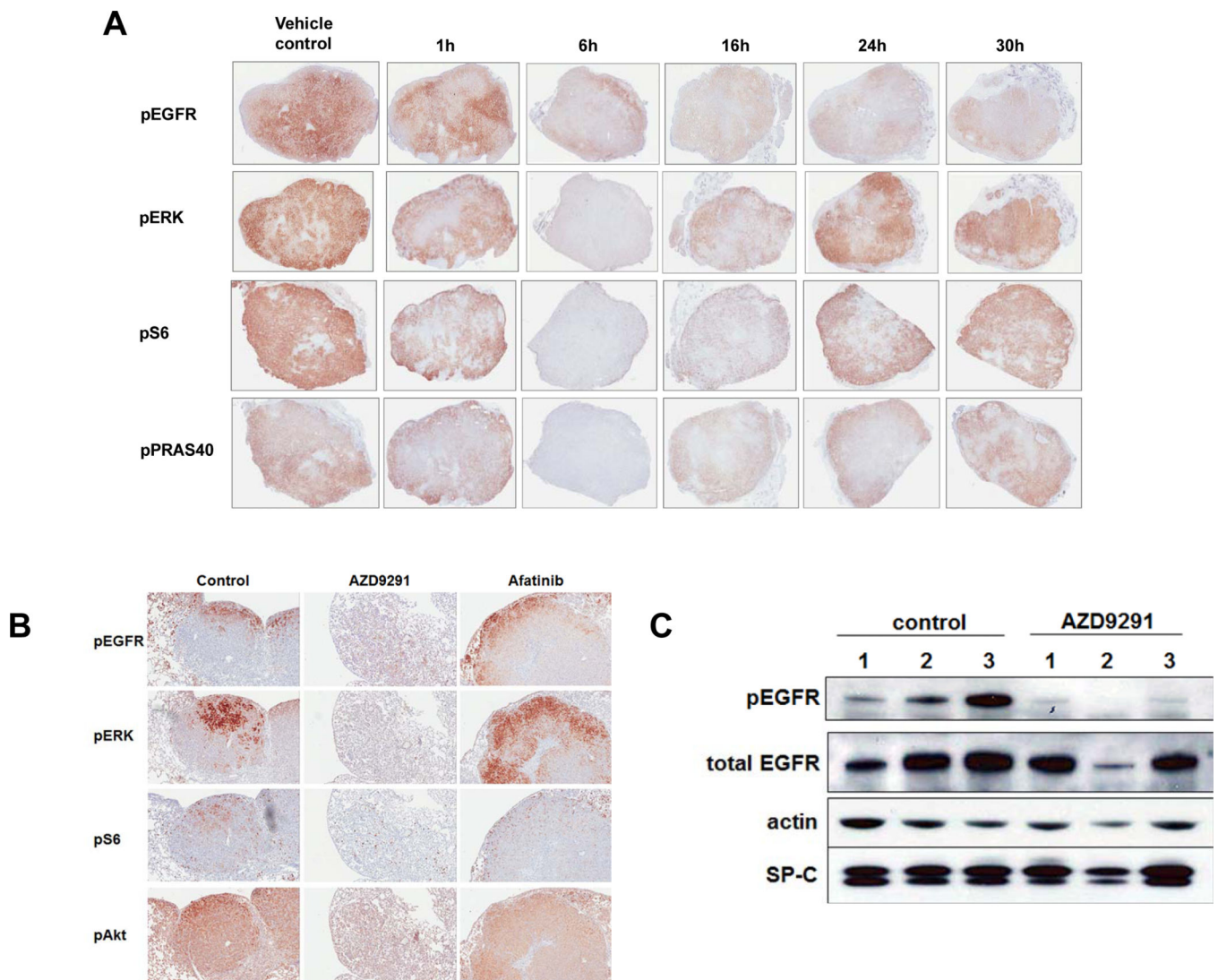
Figure 4.
In vivo anti-tumor efficacy of AZD9291 in subcutaneous xenograft models of EGFR-TKI sensitising and T790M resistant lung cancer. **A,** PC-9 (ex19del) xenograft following 14 days of daily treatment (n=6 or 8 animals depending on treatment group). **B,** H1975 (L858R/T790M) xenograft following 14 days of daily treatment (n=6 or 8 animals depending on treatment group). **C,** PC-9 following chronic daily oral dosing of 5mg/kg AZD9291 (n=8) or 6.25 mg/kg gefitinib (n=11). **D,** H1975 following chronic daily oral dosing of 1, 5 or 25 mg/kg AZD9291 (n=10 or 12 animals depending on dose group). Data are plotted as mean standard error.
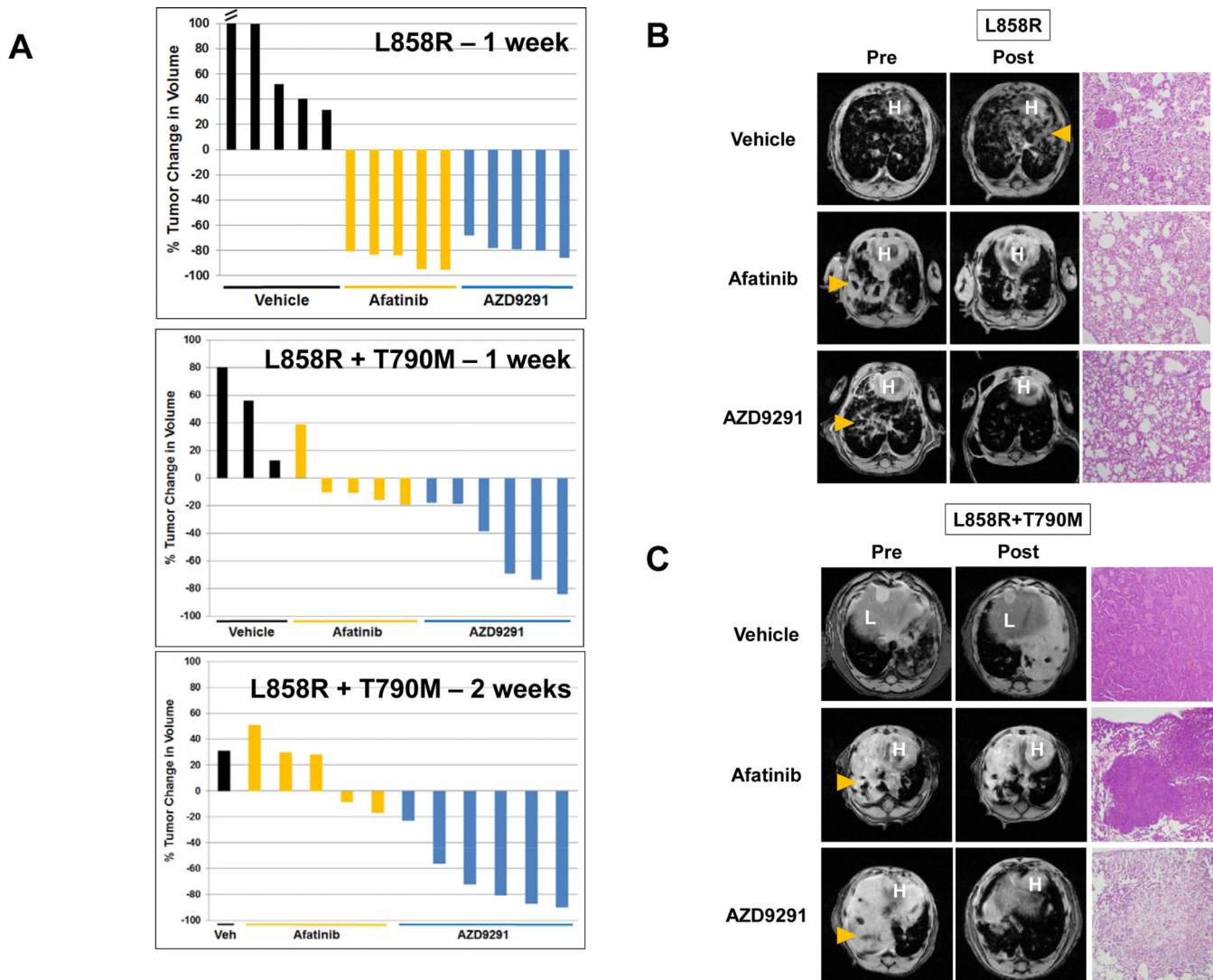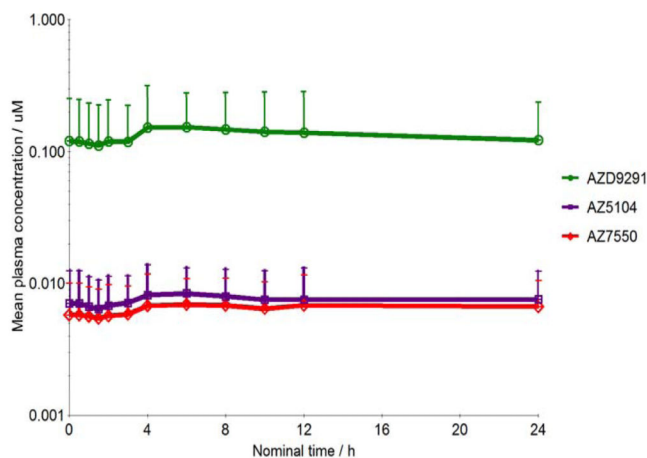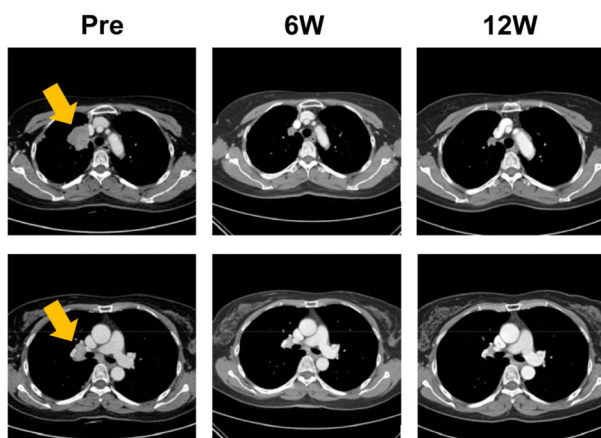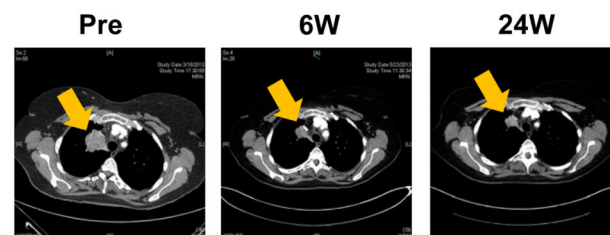
Figure 5.
AZD9291 induces significant and sustained tumor regression in transgenic models of
EGFR-TKI sensitising (C/L858R) and T790M resistant (C/L+T) lung cancer. **A,** Percent
change in radiographic tumor volume from baseline by treatment for individual lung tumor-
bearing C/L858R (top) and C/L+T (middle, bottom) animals with vehicle, afatinib (7.5
mg/kg/day), or AZD9291 (5 mg/kg/day). **B and C,** Representative MRI images and H&E
staining (original magnification, ×40) of lungs from tumor-bearing animals (**B,** C/L858R
and **C,** C/L+T) pre and post treatment with vehicle, afatinib, or AZD9291 for 1 week. H –
heart; L – liver; arrow denotes tumor.

Figure 6.

AZD9291 inhibits EGFR phosphorylation and downstream signallng in murine models of EGFR T790M resistant lung cancer. **A,** Subcutaneous H1975 (L858R/T790M) xenografts, treated with a single 5 mg/kg dose of AZD9291 for the indicated times, were examined for phospho-EGFR, -ERK, -S6, and -PRAS40 status by immunohistochemistry. Representative images were taken from scans at 20× magnification and then size adjusted to fill the screen. **B,** Lungs from representative transgenic mice treated with control, AZD9291, or afatinib were harvested 6 hours after dose administration. Formalin-fixed paraffin-embedded sections were stained with the indicated antibodies. Representative images were taken from Aperio scans at 100× magnification. **C.** Lungs were harvested from either untreated tumor-bearing transgenic mice (as confirmed by MRI) (control) or from tumor-bearing mice 8 hours after a single treatment with AZD9291 5 mg/kg. Corresponding lysates from individual animals were immunoblotted with the indicated antibodies. Anti-SP-C (surfactant protein C) antibody was used as a surrogate marker for tumor burden, as tumors express the protein.

Figure 7.
Proof of concept clinical studies validating AZD9291 as a mutant-selective EGFR kinase T790M inhibitor. **A,** Preliminary pharmacokinetic profile showing mean (+ SD) total plasma levels of AZD9291, AZ5104 and AZ7550 versus time from cohort of 6 advanced NSCLC patients. After a single dose of AZD9291 mesylate salt, followed by a 7 day washout and then 8 days of once daily 20 mg oral dosing in AURA Phase 1 study (NCT01802632). **B and C,** Serial computed tomography scans of the chest from patients before and after treatment with AZD9291 in a phase I trial. **B,** Images from a 57-year old Korean female patient diagnosed with Stage IV non-small cell lung cancer in May 2011. See main text for details. **C,** Images from a 57-year old British female never smoker diagnosed with Stage IV lung adenocarcinoma in December 2010. The patient was previously treated with first-line gefitinib for 14 months, achieving a partial response before eventually developing progressive disease. See main text for details.